Influence of aging on the resistive switching behavior of epitaxial strontium titanate based heterostructures

Vishal Sharma*[1], Sunidhi[1], Sunil K. Arora[1], F. Sánchez[2], Vinay Gupta[3] and Monika Tomar[3]

[1]*Centre for Nanoscience and Nanotechnology, Block-II, South Campus, Panjab University, Sector-25, Chandigarh-160014, India.*
[2]*Institut de Ciència de Materials de Barcelona (ICMAB-CSIC), Campus UAB, Bellaterra 08193, Spain.*
[3]*Department of Physics and Astrophysics, University of Delhi, Delhi 110007, India.*
[3]*Department of Physics, Miranda House, University of Delhi, Delhi 110007, India.*

Abstract

In this work, we investigated the impact of aging on the resistive switching behavior of high quality epitaxial heterostructure resistive switching devices [Pt/$SrTiO_3$/$LaNiO_3$/$LaAlO_3$ (001) with $SrTiO_3$ (STO) as switching layer, Pt as top electrode and $LaNiO_3$ as bottom electrode]. For this study, the resistive switching memory devices of two different ultrathin switching layer (STO) thicknesses (5 and 10 nm) were fabricated with different shape and size of top electrode (Pt) i.e. 20 µm (circular shape) and 50 µm (square shaped). Subsequently, their resistive switching behavior at different instant of time i.e. freshly prepared, 4 months and 16 months were studied. With long aging, we find a decrease in the positive bais voltages for which current start rising exponentially (set voltages) for most of the devices besides emergence of various features such as multiple crossovers, noisy/spike region during set process and openness in the switching hysteresis loop. The existence of these behaviors is attributed to the fact that the moisture permeates through the interfacial region between top electrode (Pt) and switching layer (STO) irrespective of the thickness of switching layer and dimensions of top electrode.

Keywords: Resistive Switching ; Aging ; strontium titanate heterostructures ; epitaxial thin film

1. Introduction

Functional oxide based heterostructures have emerged as main candidates for future electronics owing to surge in demand of memory applications particularly in the field of artificial intelligence, neuromorphic computing, vast memory storage devices for cloud application, etc. Strontium titanate, $SrTiO_3$ (STO) is a potential candidate for resistive switching memory applications [1,2]. It exists in the cubic crystal structure (Pm3m) with a lattice parameter of 3.905 Å, with corner- shared TiO_6 units forming the structural backbone of the lattice [3,4]. Resistive switching (RS) in oxides epitaxial heterostructure has gathered a lot of attention owing to better understanding of the dynamics associated with the oxygen vacancies and their positive impact on the resistive switching characteristics [5,6]. Bagdzevicius et al. studied the bipolar resistive switching behavior in $GdBaCo_2O_{5+\delta}/LaNiO_3$ bilayer epitaxial heterostructures [5]. They reported that the multilevel resistance states arise due to the gradual transitions in resistive switching. In another study, Nallagatla et al. investigated the resistive switching behavior in $SrFeO_{2.5}$/Nb:$SrTiO_3$ epitaxial heterostructures in two different (001) and (111) device configuration and reported that due to different oxygen vacancies dynamics under different epitaxial crystallographic orientations, resistive switching was obtained only in device with (111) configuration [6]. STO based heterostructures have also been explored as potential resistive switching memory devices which show external electric field controlled bipolar oxygen anionic

*Corres.author
E-mail:contactvishal@pu.ac.in

switching with high performance parameters i.e. R_{off} / R_{on} up to 100, endurance of 10^7 cycles and high retention time till 10^5 sec [7-11]. The core essence of switching in this material lies on the mobility of point defects, i.e. oxygen vacancies ($V_O^{\cdot\cdot}$), under an applied electric field [9-13]. These defects are primarily originated during thermal processing of the material in the oxygen deficit environment. Interestingly, changes in the resistive switching characteristics during moisture exposure were also reported [14]. This shows the induction of another conducting entity besides oxygen vacancies, which overall affect the resistive switching behavior in devices exposed to moisture conditions for shorter duration. Overall, these changes in the switching behavior highlight an important aspect related to RS mechanism i.e. quality of overall device architecture with a focus on switching layer. The good quality of device heterostructure based on STO in terms of structural, morphological and interfacial is utmost necessitate for their practical use under uncontrolled variables related to external environmental conditions. This device architecture fully supports scaling and integration with CMOS technology with due care of the practical external constraints. Moreover, with STO based epitaxial heterostructure RS devices, the mechanism of interaction between external environment conditions and device will be more simplified to understand, with minimal focus on imperfections like morphological, interfacial roughness, polycrystallinity, parasitic phases, etc. So overall, for better understanding of an interaction between external environmental conditions and memory device during long aging, a STO based epitaxial heterostructure is important.

In this work in light of above challenges, our efforts are focused on to understand the effect of aging (up to 16 months) on the resistive switching behavior of epitaxial STO based RS devices i.e. Pt/STO/$LaNiO_3$/$LaAlO_3$ (001), where Pt acts as a top electrode and $LaNiO_3$ (LNO) acts as a bottom electrode. With aging, we find a decrease in the voltages during positive bais at which current start rising exponentially (set voltages) besides emergence of multiple crossovers, noisy/spike region during set process and openness in the switching hysteresis loop. The observed features are related to the moisture induced degradation of the interfacial region between top electrode (Pt) and switching layer (STO).

2. Materials and methods

The bi-layer epitaxial heterostructure of STO (switching layer) and LNO (bottom electrode) were grown on a (100)-oriented $LaAlO_3$ (LAO) single crystalline substrate by pulsed laser deposition (PLD) using a KrF (248 nm) excimer laser. The optimized parameters used for the growth of STO and LNO over LAO were substrate temperature (700° C) and oxygen pressure of 0.2 mbar. The thickness of the LNO bottom electrode layer was 27 nm and we used STO switching layer with thickness of 5 and 10 nm. Thereafter, STO/LNO bi-layer epitaxial

heterostructures were characterized by X-ray diffraction (XRD) and atomic force microscopy (AFM). Details of growth and related characterizations can be found elsewhere [15].

The memory devices in the MIM (Metal-Insulator-Metal) planar configuration were fabricated by depositing 40 nm Platinum (Pt) top electrode by sputtering (power 10 W and Ar pressure 0.005 mbar) on STO/LNO heterostructures having STO switching layer thickness of 5 and 10 nm. Arrays of top electrodes were grown through shadow masks. We used TEM grid masks of two different shapes and size i.e. one with an array of of 50 μm squares and another with an array of 20 μm circles. The electrical characterizations of these epitaxial resistive switching devices were carried out with the help of a two probe electrical measurement (Newport Bench Top with vibration isolation system) using semiconductor characterization system (Keithley 4200-SCS). The electrical measurements were carried out in a continuous dual sweep linear mode with a voltage sweep of 50 mV. The current range of 100 pA was selected for the measurements of the switching voltages during an entire cyclic sweep.

3. Results and Discussion

Prior to discussing the resistive switching performance of the devices made from the STO/LNO/LAO heterostructures, we would like to point out that LNO grows epitaxially on LAO (001) substrate and subsequent growth of STO over LNO also occurs in an epitaxial manner [15,16]. The bi-layer epitaxial heterostructure possess a high crystalline quality as determined from XRD. Such that, θ-2θ scans as shown in the **Figure 1** confirmed c-axis oriented out of plane growth (001) of strontium titanate and lanthanum nickelate for a STO (5 nm)/LNO/LAO (001) and STO(10 nm)/LNO/LAO (001) respectively. Surface morphological analysis was carried out by AFM in a tapping mode. Topographic AFM images as shown in the **Figure 2** show the presence of small grains, 20-30 nm wide and 1-2 nm in height, likely multilayered islands. Overall the film are flat, with root mean square (rms) surface roughness below 0.6 nm (rms is 0.57 nm and 0.54 nm for STO layer thickness of 5, and 10 nm, respectively).

The resistive switching (RS) behavior of the devices (Pt/STO/LNO) made from well characterized STO/LNO bilayer heterostructure was investigated. We discuss the results on the devices made from 5 and 10 nm thick STO switching layers. For each switching layer thickness results on two devices are presented, one with square shaped top electrode (50 μm) and other one with circular shaped top electrode (20 μm). The devices on 5nm switching layer are named as S1 (50 μm square top contact) and S2 (20 μm circular top contact). The devices on 10 nm switching layer are named as S3 (50 μm square top contact) and S4 (20 μm circular top contact). We observed RS behavior in all the devices. **Figure 3** shows the resistive switching response of device S1-S4 measured at room temperature. We observed a clear bipolar resistive switching in all the devices measured. The observed set voltages is large in case of RS for smaller electrode (20 μm), with a set voltages of (1.93±0.01)V for S2 and (1.52±0.01)V for S4 respectively, as compared to bigger size (50 μm) electrodes, with a set voltages of (0.37±0.01)V for S1 and (0.26±0.01)V for S3 respectively. Asymmetric bipolar switching hysteresis curves were observed in all of the devices characterized. The asymmetry associated with the bipolar switching curve was expected, owing to the metal work function associated with the different top (Pt) and bottom (LNO) electrodes associated in the design of this heterostructure. But, interestingly for all the devices under study, Schottky behavior was observed in the switching characteristics. This Schottky behavior emerged due to the redistribution of oxygen vacancies near interfacial region on an application of external electric field and subsequently affects the induced interfacial states [18] near the surface. This has significant effect on the switching characteristics of smaller size electrode based devices (S2 and S4), where switching set and reset voltages are found to be larger as compared to bigger size electrode based devices (S1 and S3).This can be explained because of presence of induced trapped states near surface owing to modification of the work function in case of smaller electrode size based devices, the ease of formation of conducting filaments (CFs) restricted. These factors cause a rise in the respective set voltages to sustain switching mechanism. However for bigger size electrodes, gradual switching characteristics with small hysteresis and lower set voltage favorably support design of the memory devices with lower power consumption [19]. Further, we would like to state that because of the superior growth and epitaxial nature of the bilayer heterostructure, the response of the resistive switching device is expected to show less variability. Indeed, on studying their switching behavior randomly at different top contact pads of 50 μm and 20 μm respectively, almost same nature of bipolar RS cycle was observed for the different switching layer thickness of 5 nm and 10 nm **(Supplementary Figure S1)**. We found a small variation in the set voltage, possibly owing to inherent mechanism of RS involving oxygen vacancies migration under an applied electric field [18,21]. This behavior was quite expected, as surface roughness of the heterostructure

was 0.57 nm and 0.54 nm for switching layer thickness of 5 and 10 nm respectively, which favorably provide smooth surface throughout the sample with minimal surface defects for the growth of top electrodes of different sizes. So, cumulatively it provides lesser device to device variation among various devices formed from these heterostructures.

Thereafter, we studied the impact of aging on all these devices. Here, memory devices were kept in a cuvette at normal room temperature conditions over a span of 16 months. We studied the switching response of the devices after 4 months and thereafter another 12 months, with an intention of investigating any behavioral change. **Figure 4 and 5** shows the RS response of devices (S1, S2) and (S3, S4), respectively measured on freshly prepared device, after 4 month and 16 months of time. Figure 4(a) shows that after 4 months of aging the devices exhibits change in bipolar switching. It exhibits switching in the first quadrant and an open loop in the third quadrant. The RS response measured after 16months, exhibited an open hysteresis loop in the third quadrant and presence of spike/noisy region during setting phase of the RS switching in the first quadrant. These features were predominantly observed with a long aging in other devices as well. Cumulatively, overall response of the memory devices S1, S2, S3 and S4 is tabulated in the **Table 1**. Despite high quality heterostructure design, various changes observed in the RS switching characteristics with aging attract a sudden attention.

The observation of features like multiple crossovers, openness in the hysteresis loop and presence of spike/noisy region during setting phase needs attention. Several possibilities like material modification, interface alteration, trapped states, oxygen vacancies redistribution, externally induced impurity etc., are to be considered to understand the influence of aging induced additional features in the RS behavior. Firstly, we consider the material properties/degradation of STO. Being an important member of titanate perovskite family STO has been well explored for adsorption capabilities [20]. It increases the probability of their interaction with moisture present in the air (H_2O + O_2). Several oxides earlier have shown variation in their electrical properties upon exposure with moisture [22]. The adsorption sites present in the switching layer (STO) provide an active site for moisture to interact and is incorporated as a protonic ($OH^{\cdot}$) charge carrier into the bulk oxide by a well-known hydration reaction [23,24] given below :

$$H_2O + O_2 + V^{\cdot\cdot} \rightleftharpoons 2OH^{\cdot} \quad \textbf{(1)}$$

where $OH^{\cdot}$ act as protonic entity introduced in the bulk of the STO layer with a long aging and contribute in the overall conductivity of the sample [25-27] besides anionic electronic contribution via oxygen vacancies ($V^{\cdot\cdot}$). Now, here in our case, during the deposition of top electrode Pt via sputtering, as the sample was exposed to air during transfer from PLD chamber to sputtering chamber, there is a possibility of various surface defects being induced. These defects may act as permeable sites for moisture to underwent electrochemical reaction with an underlying switching layer (STO) surface and subsequently affect the RS characteristics. It was reported that exposure of moisture between Pt and material through interfacial region causes alteration in the work function [28] of the electrode which subsequently reflected in the present case with a change in set voltage. It also increase spike/noisy region in the characteristics due to induction of various trapped states near surface caused by other conducting entity i.e. protonic ($OH^{\cdot}$) entity, permeate in the material through surface adsorption as discussed above. Similar change in the resistive switching characteristics i.e. multiple crossings, noisy/spike region were also reported in a STO based thick material having same top and bottom electrode (Pt) [14], when exposed under different engineered moisture condition. Another interesting feature we observed with aging is the openness in the switching hysteresis loop. However, in earlier study related to resistive switching in the STO based material [19] a small openness in the switching hysteresis was reported under different sweep voltage (±2V, ±2.5 V) and higher sweep rate (500 mV/sec and 100 mV/sec) .They associated it to the slow kinetics of defects (oxygen vacancies) influenced by the sweep rate. But, here a wide openness in the switching hysteresis curves with a long aging is found at both higher and lower voltages i.e. ±2V and ±4V respectively at a lower sweep rate of 50mV/sec too, which suggests the role of another type of defects besides oxygen vacancies like induced protonic entities with a long moisture exposure and any extended defects present in the switching layer [29], in the overall control of the RS switching characteristics besides electrical parameters (sweep voltages and sweep rate). Subsequently, decrease in the set voltages for both of the device studied with aging were also observed possibly owing to improve conductivity with an addition of protonic entity during moisture exposure within the system [14]. So, cumulatively resistive switching characteristics underwent various interesting changes in terms of switching behavior and set voltages during long aging under normal environmental conditions.

4. Conclusion

We studied the influence of aging on the resistive switching response of device made from STO/LNO epitaxial heterostructures having two different switching STO layer thickness of 5 and 10 nm, and two different shape and size of top electrodes (50 µm (square shape) and 20 µm (circular shape)). All the freshly grown devices exhibited lesser switching voltage variation within devices of same dimension and topology of top Pt electrode with a complete hysteresis cycle. With aging, we observed different features such as multiple crossovers, wide open hysteresis loop, noisy/spike region and change in set voltage. We attribute the observed features to the permeation of moisture through interfacial region during long aging between switching layer (STO) and Pt electrodes. It led to induction of another conducting entity i.e. protonic ($OH^{\cdot}$), besides oxygen vacancies in the switching layer system. Thus overall, these conducting entities induce surface trapped states and alter metal work function, which affect the resistive switching characteristics with aging. Thus, inserting a suitable capping layer while the electrode designing of the heterostructure RS devices will provide better results in the future.

Acknowledgements

This project has received funding from EU-H2020 research and innovation programme under grant agreement No. 654360 within NFFA- Europe transnational access activity. We also thanks, Dr. Ignasi Fina ICMAB-CSIC for initial electrical measurement support and group members of EMDL DU for providing technical support during electrical characterization. Vishal Sharma expresses his gratitude to Panjab University, Chandigarh and thereafter UGC-DAE CSR Indore for providing fellowship for carrying out research work. Ms. Sunidhi expresses her thanks to UGC, New Delhi for providing fellowship for research work. F. Sánchez acknowledges financial support from the Spanish Ministry of Science and Innovation, through the MAT2017-85232-R (AEI/FEDER, EU), PID2020-112548RB-I00 (AEI/FEDER, EU), and Severo Ochoa FUNFUTURE (CEX2019-000917-S) projects, and from Generalitat de Catalunya (2017 SGR 1377).

References

1. T. Wan, B. Qu, H. Du, X. Lin, Q. Lin, D.W. Wang, C. Cazorla, S. Li, S. Liu, D. Chu, J. Colloid Interface Sci , 512 (2018) 767–774.
2. M. Kubicek, S. Taibl, E. Navickas, H. Hutter, G. Fafilek, J. Fleig, J Electroceram, 39 (2017) 197–209.
3. P. Chen, M. P. Cosgriff, Q. Zhang, S. J. Callori, B. W. Adams, E. M. Dufresne, M. Dawber, and P. G. Evans, Phys. Rev. Lett. 110 (2013) 047601(1-5).
4. B. L. Phoon, C. W. Lai, J. C. Juan, P. L. Show, W.H. Chen, Int J Energy Res. (2019) 1–24.
5. S. Bagdzevicius, M. Boudard, J. M. Caicedo, X. Mescot, R. R. Lamas, J. Santiso, M. Burriel, Solid State Ion., 334 (2019) 29–35.
6. V. R. Nallagatla and C. U. Jung, Appl. Phys. Lett. 117 (2020) 143503 (1-6).
7. K. Szot, R. Dittmann, W. Speier and R. Waser, Phys. Status Solidi (RRL) 1 (2007) R86–R88.
8. D. J. Seong , M. Jo , D. Lee , H. Hwang, Electrochem. Solid State Lett.**,** *10* (2007) H168-H170 .
9. D. Panda , T. Y. Tseng, Ferroelectrics 471 (2014) 23-64 .
10. X. Guo, Appl. Phys. Lett., 101(2012) 152903(1-4) .
11. S. Menzel , M. Waters , A. Marchewka , U. Bottger , R. Dittmann , R. Waser*,* Adv. Funct. Mater., 21 (2011) 4487-4492 .
12. R. Waser , R. Dittmann , G. Staikov , K. Szot, Adv. Mater., 21 (2009) 2632-2663.
13. H. Akinaga , H. Shima*, Proc. IEEE*, *98* (2010) 2237-2251.
14. F. Messerschmitt, M. Kubicek and J. L. M. Rupp, Adv. Funct. Mater. 25 (2015) 5117–5125.
15. F. Sanchez, C. Ferrater, C. Guerrero, M.V. García-Cuenca, M. Varela, Appl. Phys. A, 71 (2000) 59–64.
16. M. C. Weber, M. Guennou, N. Dix, D. Pesquera, F. Sánchez, G. Herranz, J. Fontcuberta, L. López-Conesa, S. Estradé, F. Peiró, J. Ĩniguez and J. Kreisel, Phys. Rev.B, 94 (2016) 014118 (1-11).
17. N. H. Cho, S.H. Nam, and H.G.Kim, J.Vac.Sci.Technol.A, 10(1) (1992) 87-91.
18. H. Stöcker, M. Zschornak, J. Seibt, F. Hanzig, S. Wintz, B. Abendroth, J. Kortus, D. C. Meyer, Appl. Phys. A 100 (2010) 437–445.
19. Y. Qi, Z. Shen, C. Zhao, C. Z. Zhao, J. Alloys Compd. Volume 822 (2020) 153603 (1-10).

20. U. Terranova, F. Vi˜nes, N. H. d. Leeuw and F. Illas, J. Mater. Chem. A, 8 (2020) 9392-9398.
21. F. Messerschmitt , M. Kubicek , S. Schweiger , J. L. M. Rupp, Adv. Funct. Mater., 24 (2014) 7448-7460.
22. T. Seiyama , N. Yamazoe , H. Arai, *4* (1983) 85-96.
23. S. Steinsvik , Y. Larring , T. Norby , Solid State Ionics,143 (2001) 103-116.
24. R. Waser, Phys. Chem., 90 (1986) 1223-1230.
25. W. Qu , R. Green , M. Austin**,** Meas. Sci. Technol. 11 (2000**)** 1111-1118.
26. Y. Yamazaki , P. Babilo , S. M. Haile**,** Chem. Mater. 20 (2008) 6352-6357.
27. R. B. Cervera , Y. Oyama , S. Miyoshi , I. Oikawa , H. Takamura , S. Yamaguchi , Solid State Ionics, 264 (2014) 1-6.
28. S. Hirose, S. Ueda, N. Ohashi, J.Appl.Phys.125 (2019) 095301 (1-10).
29. C. Rodenbücher, S. Menzel, D. Wrana, T. Gensch, C. Korte, F. Krok, K. Szot, Sci Rep 9 (2019) 1-9.

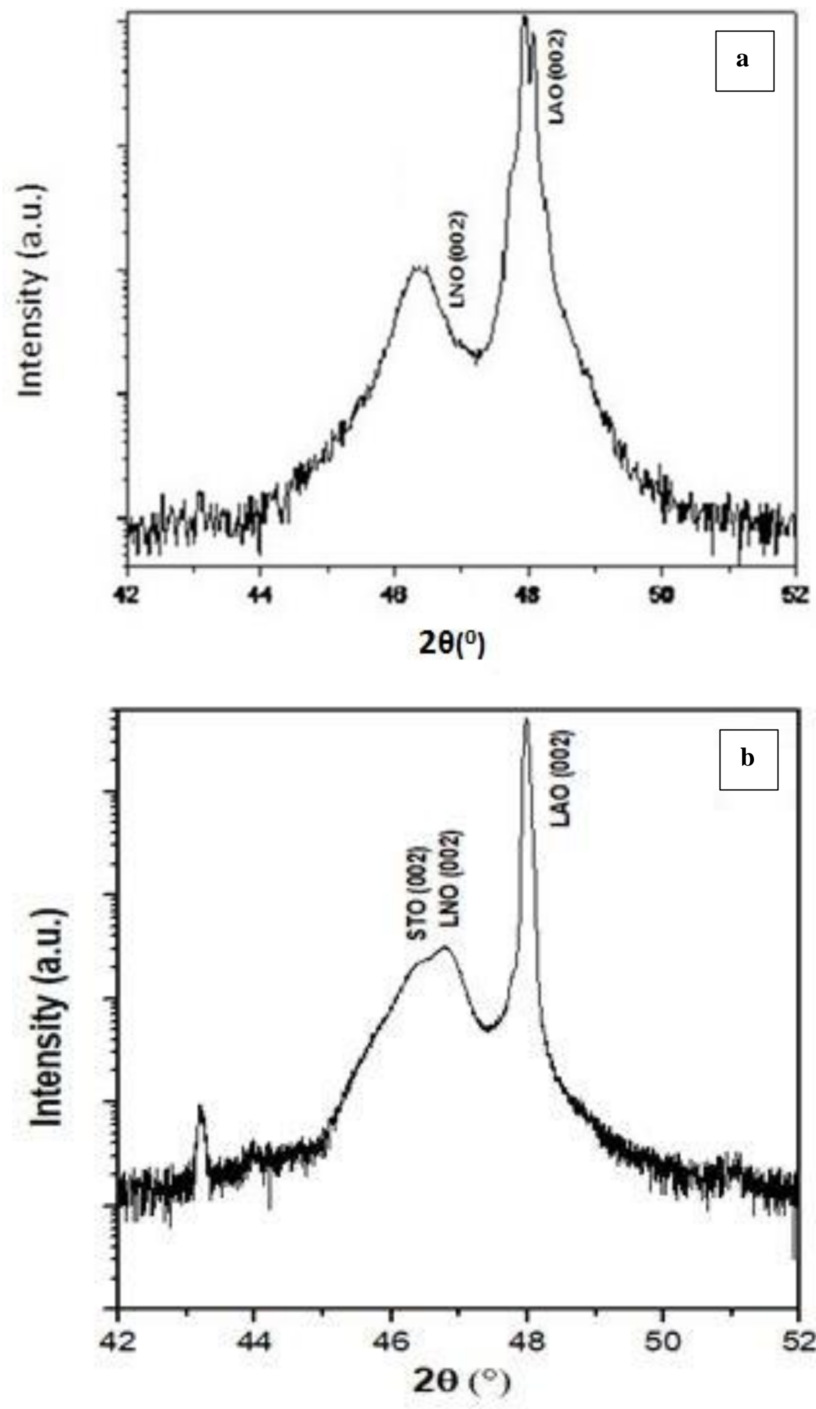

Figure 1. XRD θ-2θ scan of the, **a**. STO (5 nm)/LNO/LAO(001) and **b.** STO (10 nm)/LNO/LAO(001)samples.

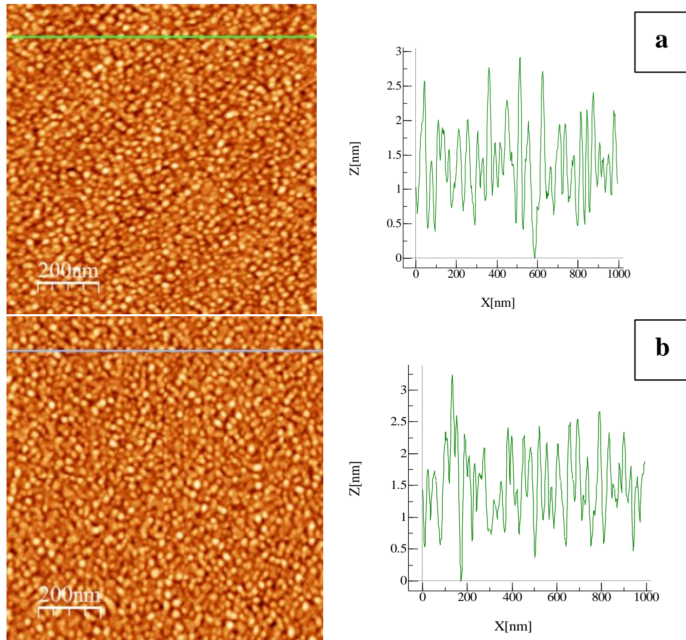

Figure 2. Topographic atomic force microscopic image (1×1 µm^2) of the, (**a**) STO (5 nm)/LNO/LAO (001) and (**b**) STO (10 nm)/LNO/LAO (001) samples. **Right panel**: Height profile along the horizontal line shown in the images.

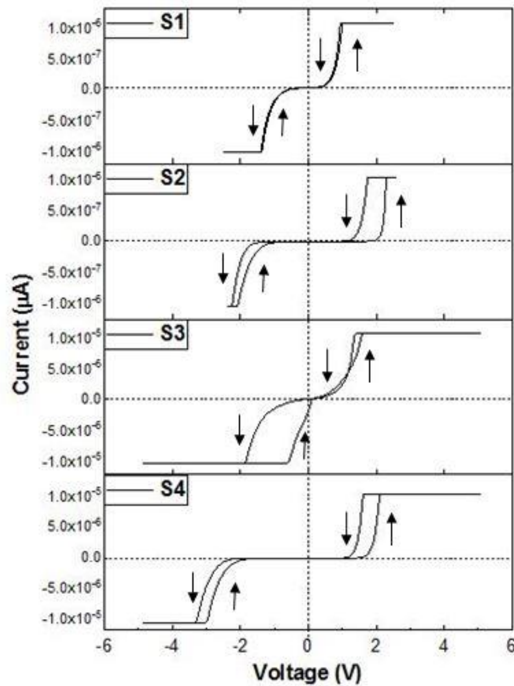

Figure 3. Resistive switching response in the bi-layer epitaxial heterostructure of STO/LNO/LAO with STO = 5 and 10 nm, such that at STO = 5nm such that at STO = 5nm, **S1 and S2** shows switching curve at square and circular shaped top electrodes respectively, whereas for STO =10 nm, **S3 and S4** shows switching curve at square and circular shaped top electrodes respectively.

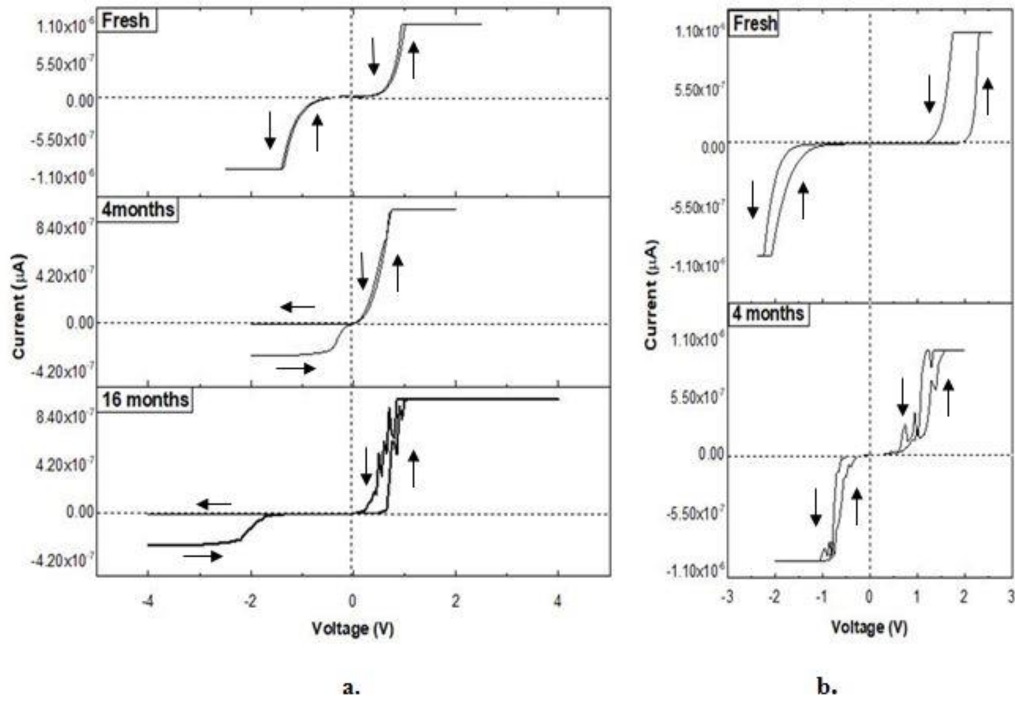

Figure 4. Aging effect on the resistive switching response in **S1 and S2**, a bi-layer epitaxial heterostructure of STO/LNO/LAO with STO = 5 nm, such that, **a**. S1, shows behavioral change in the resistive switching at square shaped top electrode **b**. S2, shows behavioral change in the resistive switching at circular shaped top electrode.

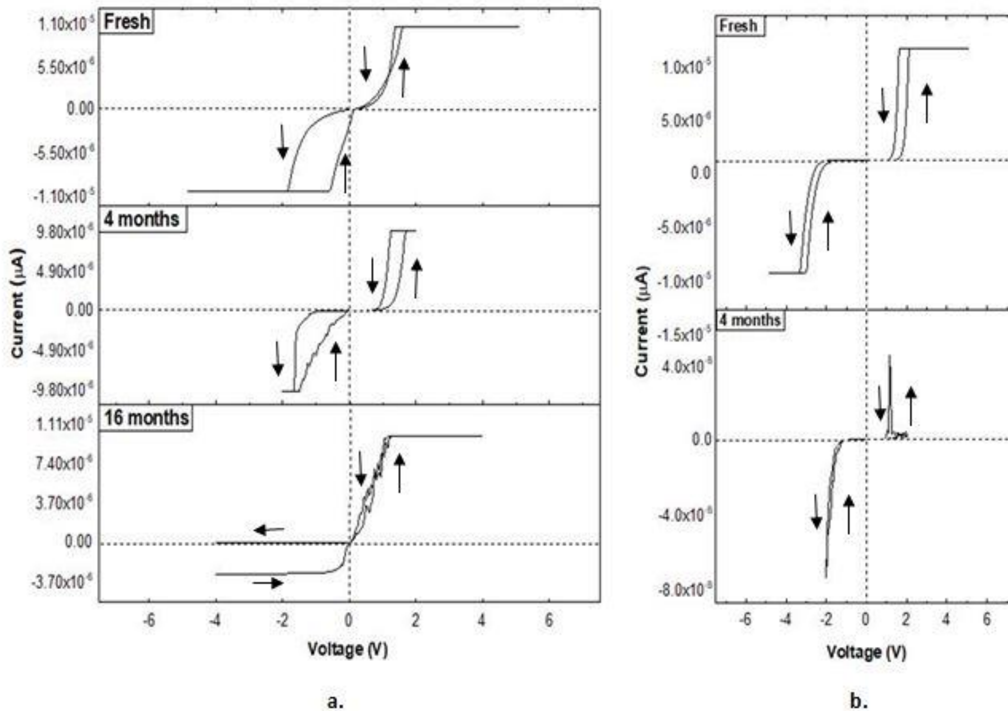

Figure 5. Aging effect on the resistive switching response in **S3 and S4**, a bi-layer epitaxial heterostructure of STO/LNO/LAO with STO = 10 nm, such that, **a**. S3, shows behavioral change in the resistive switching at square shaped top electrode **b**. S4, shows behavioral change in the resistive switching at at circular shaped top electrode.

Supplementary

Influence of aging on the resistive switching behavior of epitaxial strontium titanate based heterostructures

Vishal Sharma*[a], Sunidhi[a], Sunil K. Arora[a], F. Sánchez[b], Vinay Gupta[c] and Monika Tomar[d]

[a]*Centre for Nanoscience and Nanotechnology, Block-II, South Campus, Panjab University, Sector-25, Chandigarh-160014, India.*
[b]*Institut de Ciència de Materials de Barcelona (ICMAB-CSIC), Campus UAB, Bellaterra 08193, Spain.*
[c]*Department of Physics and Astrophysics, University of Delhi, Delhi 110007, India.*
[d]*Department of Physics, Miranda House, University of Delhi, Delhi 110007, India.*

* Corresponding author: contactvishal@pu.ac.in

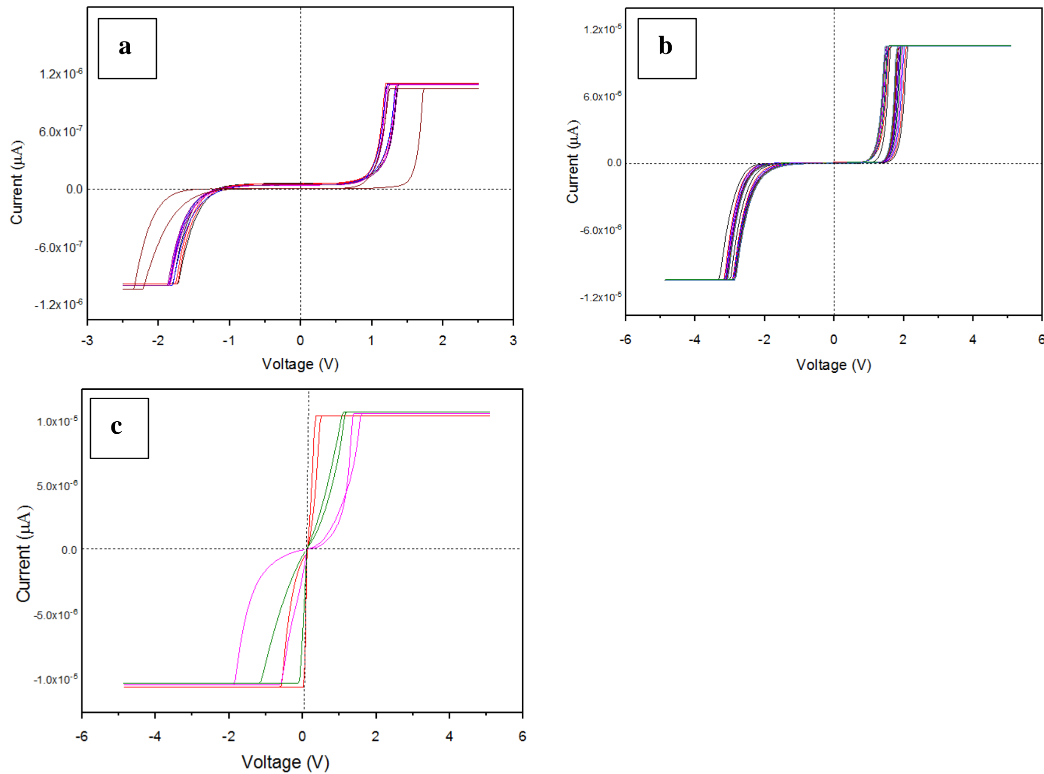

Figure 1. Resistive switching response in the **a.** STO (5 nm)/LNO/LAO(001) sample, at different Pt contact pads of size 20 µm, **b.** STO (10 nm)/LNO/LAO(001) sample, at different Pt contact pads of size 20 µm and **c.** STO (10 nm)/LNO/LAO(001) sample, at different Pt contact pads of size 50 µm.